THE JOURNAL OF BIOLOGICAL CHEMISTRY VOL. 285, NO. 34, pp. 26174–26181, August 20, 2010

Transmembrane Protein 147 (TMEM147) Is a Novel Component of the Nicalin-NOMO Protein Complex*[S]

Received for publication, April 9, 2010, and in revised form, June 1, 2010 Published, JBC Papers in Press, June 10, 2010, DOI 10.1074/jbc.M110.132548

Ulf Dettmer[‡], Peer-Hendrik Kuhn[‡], Claudia Abou-Ajram[‡], Stefan F. Lichtenthaler[‡], Marcus Krüger[§], Elisabeth Kremmer[¶], Christian Haass[‡], and Christof Haffner[‡1]

From the [‡]German Center for Neurodegenerative Diseases (DZNE) and the Adolf-Butenandt-Institute, Biochemistry, Ludwig-Maximilians-University, D-80336 Munich, the [§]Max-Planck-Institute for Heart and Lung Research, D-61231 Bad Nauheim, and the [¶]Helmholtz Zentrum, Institute of Molecular Immunology, D-81377 Munich, Germany

Nicastrin and its relative Nicalin (Nicastrin-like protein) are both members of larger protein complexes, namely γ-secretase and the Nicalin-NOMO (Nodal modulator) complex. The γ-secretase complex, which contains Presenilin, APH-1, and PEN-2 in addition to Nicastrin, catalyzes the proteolytic cleavage of the transmembrane domain of various proteins including the β-amyloid precursor protein and Notch. Nicalin and its binding partner NOMO form a complex that was shown to modulate Nodal signaling in developing zebrafish embryos. Because its experimentally determined native size (200–220 kDa) could not be satisfyingly explained by the molecular masses of Nicalin (60 kDa) and NOMO (130 kDa), we searched in affinity-purified complex preparations for additional components in the low molecular mass range. A ~22-kDa protein was isolated and identified by mass spectrometry as transmembrane protein 147 (TMEM147), a novel, highly conserved membrane protein with a putative topology similar to APH-1. Like Nicalin and NOMO, it localizes to the endoplasmic reticulum and is expressed during early zebrafish development. Overexpression and knockdown experiments in cultured cells demonstrate a close relationship between the three proteins and suggest that they are components of the same complex. We present evidence that, similar to γ-secretase, its assembly is hierarchical starting with the formation of a Nicalin-NOMO intermediate. Nicalin appears to represent the limiting factor regulating the assembly rate by stabilizing the other two components. We conclude that TMEM147 is a novel core component of the Nicalin-NOMO complex, further emphasizing its similarity with γ-secretase.

γ-Secretase is an intramembrane-cleaving proteolytic complex for which a variety of substrates have been identified, most importantly the transmembrane receptor Notch and the Alzheimer disease-associated β-amyloid precursor protein (1, 2). This complex consists of four transmembrane proteins including Presenilin 1 or 2, which are the enzymatically active components (3), Nicastrin (4), PEN-2 and APH-1 (5, 6). Nicastrin contains an aminopeptidase-like domain that has been suggested to be involved in γ-secretase maturation and substrate recognition (7–9). We have previously found that this domain is most closely related to the aminopeptidase-like domain of a novel protein that we named Nicalin (Nicastrin-like protein) and that is also part of a membrane protein complex (10). This complex localizes to the endoplasmic reticulum (ER)[2] membrane and also contains the 130-kDa protein NOMO (Nodal modulator). It has been shown to interfere with early development in zebrafish embryos by modulating the Nodal/transforming growth factor β pathway. Unlike γ-secretase, no proteolytic activity has been detected for the Nicalin-NOMO complex, and its molecular mode of action is unknown (10).

The cellular expression levels of both γ-secretase and the Nicalin-NOMO complex are limited by a posttranscriptional regulation mechanism that originates from the assembly of the complexes (11–15). While unassembled monomeric components are unstable and rapidly degraded, their incorporation into the complex results in their stabilization, leading to a significant increase of their half-lives. In the case of γ-secretase, the assembly occurs in a stepwise manner (16, 17), initiated by the formation of an APH-1-Nicastrin subcomplex, which serves as scaffold for the interaction and stabilization of the Presenilin holoprotein (18). Upon incorporation of PEN-2, Presenilin undergoes autoproteolysis into an N- and a C-terminal fragment (18), and the fully assembled complex is released from the ER (19, 20). No proteolytic processing of Nicalin or NOMO has been observed, and the assembly mode of their complex is less well understood. However, our recent overexpression and knockdown experiments showed that Nicalin, like Nicastrin, plays a crucial role in complex assembly by controlling the cellular steady-state levels of NOMO (11). This similarity raised the question whether the Nicalin-NOMO complex might be

* This work was supported by the Deutsche Forschungsgemeinschaft (Leibniz Award to C. Haass, Sonderforschungsbereich 596 to C. Haass and S. F. L.), the Bundesministerium für Bildung und Forschung (BMBF) through the competence network "Degenerative dementias" (to S. F. L. and C. Haass), the Centre for Integrated Protein Science Munich, a Ph.D. scholarship of the "Stiftung Stipendien-Fonds des Verbandes der chemischen Industrie" (to U. D.), and a "Forschungsprofessur" of the Ludwig-Maximilians-University (to C. Haass).

[S] The on-line version of this article (available at http://www.jbc.org) contains supplemental Fig. 1.

[1] To whom correspondence should be addressed: Institute for Stroke and Dementia Research, Klinikum Grosshadern, Ludwig-Maximilians-University, Max-Lebsche-Platz 30, D-81377 Munich, Germany. Tel: 49-089-7095-8352; E-mail: chaffner@med.uni-muenchen.de.

[2] The abbreviations used are: ER, endoplasmic reticulum; Ncl, Nicalin, Nicastrin-like protein; NOMO, Nodal modulator; T147, TMEM147, transmembrane protein 147; RNAi, RNA interference; HEK, human embryonic kidney; DDM, *n*-dodecyl-β-D-maltoside; nAChR, nicotinic acetylcholine receptor; CHAPS, 3-[(3-cholamidopropyl)dimethylammonio]-1-propanesulfonate; BisTris, 2-[bis(2-hydroxyethyl)amino]-2-(hydroxymethyl)propane-1,3-diol; LC, liquid chromatography; MS, mass spectrometry; MS/MS, tandem MS; ce, *Caenorhabditis elegans*; zf, zebrafish.

more similar to γ-secretase than previously thought and whether it could contain unidentified components, which we might have missed previously. This idea was supported by the discrepancy between the native molecular size of the Nicalin-NOMO complex as determined by Blue-Native-PAGE (200–220 kDa) and the combined molecular sizes of monomeric Nicalin (60 kDa) and NOMO (130 kDa) (11). We, therefore, explored this possibility by optimizing the Nicalin affinity purification procedure used previously to co-purify NOMO (10) and searched for specific binding partners in the low molecular mass range. An ~22-kDa band was consistently enriched in these preparations and could be identified as transmembrane protein 147 (TMEM147) by mass spectrometry analysis. The biochemical characterization of this factor and the analysis of its relationship to Nicalin and NOMO led us to the conclusion that it represents a third core component of the complex.

EXPERIMENTAL PROCEDURES

Cloning of TMEM147 cDNAs—Human TMEM147 (T147) cDNA was amplified using cDNA from human embryonic kidney 293T (HEK293T) cells and the primers T147F (5′-GCGAATTCGGCATCATGACCCTGTTT-3′) and T147R (5′-GCCTCGAGATAGGAGTGCACATTGACAAC-3′). It was cloned into the pcDNA6/V5-His A vector (Invitrogen) using EcoRI and XhoI restriction sites. Zebrafish TMEM147 (zfT147) was amplified using cDNA isolated from day 1 zebrafish embryos and the primers zfT147F (5′-GCGAATTCACCATGACTCTTTTTTCA-3′) and zfT147R (5′-GCCTCGAGGTTGCTGTGGACGA-3′). It was cloned into the vectors pCDNA4/TO/Myc-His (Invitrogen) and pCS2+ (21) using EcoRI and XhoI restriction sites. Nicalin truncation constructs NclΔC-Myc and NclΔTMC encoding amino acids 1–549 and 1–525 were cloned into pCDNA4/TO/Myc-His. The analogous Nicalin knockdown rescue constructs NclΔCmut (untagged) and NclΔTMCmut contained silent mutations at the siRNA binding site and were cloned into pcDNA6/V5-His A.

Antibodies—The monoclonal anti-Nicalin antibody NiNT was generated by immunizing rats with a peptide containing amino acids 43–58 (AHEFTVYRMQQYDLQGC), and hybridoma cell supernatants were used 1:400 for immunoblotting, 1:50 for immunoprecipitation, and undiluted for immunofluorescence. The monoclonal anti-NOMO antibody NOM4A12 was generated by immunizing rats with a peptide containing amino acids 923–938 (CQYYFKPMMKEFRFEPS), and hybridoma cell supernatants were used 1:5 for immunoblotting. The monoclonal anti-TMEM147 antibody T147.11 was generated by immunizing mice with a peptide containing amino acids 124–140 (RGIEFDWKYIQMSIDSNC), and hybridoma cell supernatants were used 1:7 for immunoblotting. The following other antibodies were used: monoclonal anti-Myc (9E10, Hybridoma Bank, Iowa University), monoclonal anti-V5 (Invitrogen), polyclonal anti-calnexin (StressGen), monoclonal anti-β-actin (Sigma), and monoclonal anti-β-catenin (Sigma).

Cell Lines and Transfection—HEK293T, T-REx-293 (293TR) cells (Invitrogen), and human cervix carcinoma HeLa cells were cultured in Dulbecco's modified Eagle's medium with GlutaMAX (Invitrogen) supplemented with 10% fetal calf serum and 1× penicillin/streptomycin. Transfections were carried out using Lipofectamine 2000 (Invitrogen), and stable cell clones were selected using either zeocin (200 μg/ml) or blasticidin (10 μg/ml). The expression of Nicalin in T-REx-293 cells was induced with 0.1 μg/ml tetracycline.

Mass Spectrometry—Enhanced liquid chromatography-mass spectrometry (GeLC-MS) was essentially performed as described (22). In brief, proteins were separated on a NuPAGE 4–12% BisTris gel (Invitrogen), and after staining with Coomassie Brilliant Blue G-250 (PageBlue, Fermentas), bands of interest were cut out. Proteins within gel pieces were subjected to reduction and alkylation followed by trypsin cleavage. Subsequently, peptides were extracted as described (23) and desalted as well as concentrated using Stage Tips. Reverse phase nano-LC-MS/MS was performed on an Agilent 1200 nanoflow LC system (Agilent Technologies), which was coupled online to a LTQ-Orbitrap (Thermo Scientific) equipped with a nanoelectrospray source (Proxeon). For the identification of proteins, the MASCOT database was searched using the following parameters: maximum of two missed trypsin cleavages, cysteine carbamidomethylation, methionine oxidation, and N-terminal protein acetylation. The obtained data were confirmed by matrix-assisted laser desorption/ionization (MALDI-TOF) peptide mass fingerprinting.

Fish Strains and Whole-mount in Situ Hybridization—Experiments were carried out using the wild-type zebrafish line AB in compliance with the guidelines of the Bavarian Council on Animal care. Fish were maintained, raised, and mated as described (24). Embryos were kept at 28 °C and staged as described (25). mRNA *in situ* hybridization was carried out as described (26) with the NotI-linearized vector pCS2+/MEM as template for cRNA probe synthesis using the DIG RNA labeling kit SP6/T7 (Roche Applied Science). Day 2 fish were bleached prior to *in situ* hybridization by incubation in 3% H_2O_2, 0.5% KOH.

Polyacrylamide Gel Electrophoresis and Immunoprecipitation—Membrane protein lysates were prepared by hypotonically lysing cells in 50 mM sodium citrate, pH 6.4, 1 mM EDTA, 1× protease inhibitor mix (Roche), pelleting cell membranes from the postnuclear supernatant fraction for 30 min at 16,000 × *g*, and solubilizing them in 50 mM Tris, pH 7.6, 150 mM NaCl, 2 mM EDTA containing 0.7% dodecyl-β-D-maltoside (DDM) or 1% Nonidet P-40 and 1× protease inhibitor mix. Insoluble components were pelleted for 10 min at 16,000 × *g*.

For immunoprecipitation, lysates were precleared by the addition of protein G-Sepharose (GE Healthcare) and shaking at 4 °C for a minimum of 2 h. To 1 mg of the precleared lysates, 2 μg of anti-Myc antibody, 1 μg of anti-V5 antibody, or 10 μl of NiNT hybridoma supernatant were added followed by incubation for 2 h at 4 °C. Subsequently, 10 μl of protein G-Sepharose per 1 mg of lysate were added, again followed by incubation for 2 h at 4 °C. Beads with bound material were washed three times by adding 200 μl of lysis buffer and immediate centrifugation for 2 min at 1000 × *g*. SDS-PAGE and immunoblotting were carried out as described (14) except that protein lysates were heated only to 60 °C to avoid aggregation of TMEM147.

Immunofluorescence Microscopy—Cells were grown on poly-L-lysine-coated coverslips, fixed 20 min with phosphate-buffered saline, 3.7% paraformaldehyde, permeabilized 20 min with

phosphate-buffered saline, 0.2% Triton X-100, and blocked 1 h with phosphate-buffered saline, 1% bovine serum albumin. Antibody incubations were performed for 1 h at room temperature in phosphate-buffered saline using a humid chamber. For detection, Alexa Fluor 488- and Alexa Fluor 555-coupled secondary antibodies (Molecular Probes) were used, and after mounting the samples in Mowiol (Hoechst), they were analyzed with a Zeiss Axioplan fluorescent microscope.

Subcellular Fractionation—Subcellular fractionation was carried out as described previously (11).

RNA Interference and Lentiviral Infection—The Nicalin- and NOMO-specific target sequences used in the RNA interference (RNAi) studies have been described (11). As TMEM147-specific target sequence, we chose CTGCTTCGCTCTTGCCTACTT. For expression of the respective short hairpin RNAs, the pLVTHM vector (27) was used, which had been modified by inserting the H1 promoter. Annealed oligonucleotides (purchased from Thermo Electron, Ulm, Germany) were cloned into pLVTHM using MluI/XmaI sites. TMEM147mut-V5 harboring silent mutations at the TMEM147 siRNA targeting site was amplified by PCR and cloned into the FU-ΔZeo vector using BamH1/NotI sites. FU-ΔZeo was generated from the FUGW vector (28) by exchange of green fluorescent protein for a multiple cloning site and removal of the Zeocin resistance. To generate stable knockdown cells, lentiviral supernatants were produced by transfecting low passage HEK293T cells with psPAX2 (Addgene, plasmid 12260), pcDNA3.1(−)-VSV-G (generated from pCMV-VSV-G, Addgene plasmid 8454), and pLVTHM-TMEM147, -Nicalin, or -NOMO. After overnight incubation, the medium was filtered through a 0.45-μm sterile filter and added to HeLa cells to obtain stable short hairpin RNA-producing cell pools. The procedure for the generation of TMEM147 rescue cells was identical except that for the transfection, the FUΔZeo-TMEM147mut-V5 vector was used instead of pLVTHM-TMEM147.

Quantitative Real-time PCR—Total RNA from HEK293T cells and stably transfected cell lines was isolated using the RNeasy Kit (Qiagen), and 4 μg were used for the synthesis of cDNA using oligo(dT) primers and the SuperScript first-strand synthesis system (Invitrogen). 2.5% of the cDNA were used for a SYBR Green real-time PCR reaction (40 cycles with 15 s at 95 °C and 60 s at 65 °C) on a Bio-Rad IQ5 machine using described primers for Nicalin and NOMO (11) and T147F and T147R (see above) for TMEM147. Reactions were performed in triplets, and the obtained CT values were normalized to β-actin expression by the comparative CT method.

RESULTS

TMEM147 Co-purifies with the Nicalin-NOMO Complex—To search for additional components of the Nicalin-NOMO complex, we modified the Nicalin affinity purification procedure, which had led to the identification of NOMO (10), most importantly by the use of DDM instead of CHAPS as detergent to solubilize membrane proteins. DDM has been used to purify the γ-secretase complex (29) and also allows the isolation of the Nicalin-NOMO complex. Using the modified protocol, a 22-kDa band was specifically enriched in preparations from Nicalin-Myc-overexpressing cells (Fig. 1*A*, *left panel*). After in-gel trypsin digestion and generation of peptide mass fingerprints by LC-MS/MS analysis, this protein was identified as TMEM147, an uncharacterized protein of 224 amino acids, also known as Nifie14. Like Nicalin and NOMO, it is highly conserved and appears to be ubiquitously expressed according to databases (GeneNote). With its seven transmembrane domains (predicted by the PRODIV-TMHMM model (30)), TMEM147 is highly hydrophobic and largely embedded within the membrane.

To validate the identity of TMEM147 and its association with the Nicalin-NOMO complex, we cloned the human cDNA from HEK293T cells and generated a monoclonal antibody using a synthetic peptide as antigen (see "Experimental Procedures"). It recognizes a band of ~22 kDa in wild-type cells (Fig. 1*A*, *right panel*) and a band of ~25 kDa in cells overexpressing a V5-tagged TMEM147 construct (Fig. 1*B*, *right panel*). Its specificity is further demonstrated by the reduction of the ~22-kDa band in cells expressing TMEM147-specific short hairpin RNAs (see below). Using this antibody, we confirmed the enrichment of TMEM147 in Nicalin immunoprecipitates (Fig. 1*A*, *right panel*). When V5-tagged TMEM147 was immunoprecipitated from overexpressing cells, a specific enrichment of 60- and 130-kDa proteins representing Nicalin and NOMO was observed (Fig. 1*B*). Moreover, an analysis of the post-immunoprecipitation material showed an efficient depletion of all three proteins after Nicalin or TMEM147 precipitation (Fig. 1*C*). These data suggested a specific interaction between TMEM147, Nicalin, and NOMO and indicated that TMEM147 might indeed represent a novel component of the complex.

TMEM147 Colocalizes with Nicalin and NOMO in the Endoplasmic Reticulum (ER)—Because the Nicalin-NOMO complex localizes to the ER membrane (10), we examined the distribution of TMEM147 in cultured cells. The subcellular localization of glycoproteins like Nicalin and NOMO can be determined by analyzing their asparagine (*N*)-linked glycans that undergo maturation during the passage through the secretory pathway. Deglycosylation experiments using *N*-glycosidase F, however, revealed no shift of the apparent molecular weight of TMEM147, suggesting that it does not contain *N*-linked carbohydrates, in agreement with the lack of *N*-glycosylation motifs within its amino acid sequence (data not shown). We, therefore, performed fractionation of cellular membranes using density gradient centrifugation followed by immunoblot detection. Like Nicalin and NOMO, TMEM147 was present exclusively in the four bottom fractions, which are enriched for ER membranes as demonstrated by the presence of the ER marker calnexin and immature Nicastrin (Fig. 2*A*). Fraction four also contained membranes from the early Golgi compartment, where the maturation of the *N*-linked carbohydrates of Nicastrin occurs. To confirm this result, we used immunofluorescence microscopy in HeLa cells, where endogenous Nicalin can be detected using a recently generated monoclonal anti-Nicalin antibody (see "Experimental Procedures") (Fig. 2*B*). Co-staining experiments revealed a high degree of overlap with calnexin, confirming the ER localization of Nicalin reported earlier (11). Highly similar patterns were also obtained by co-staining for Nicalin and TMEM147 in cells expressing

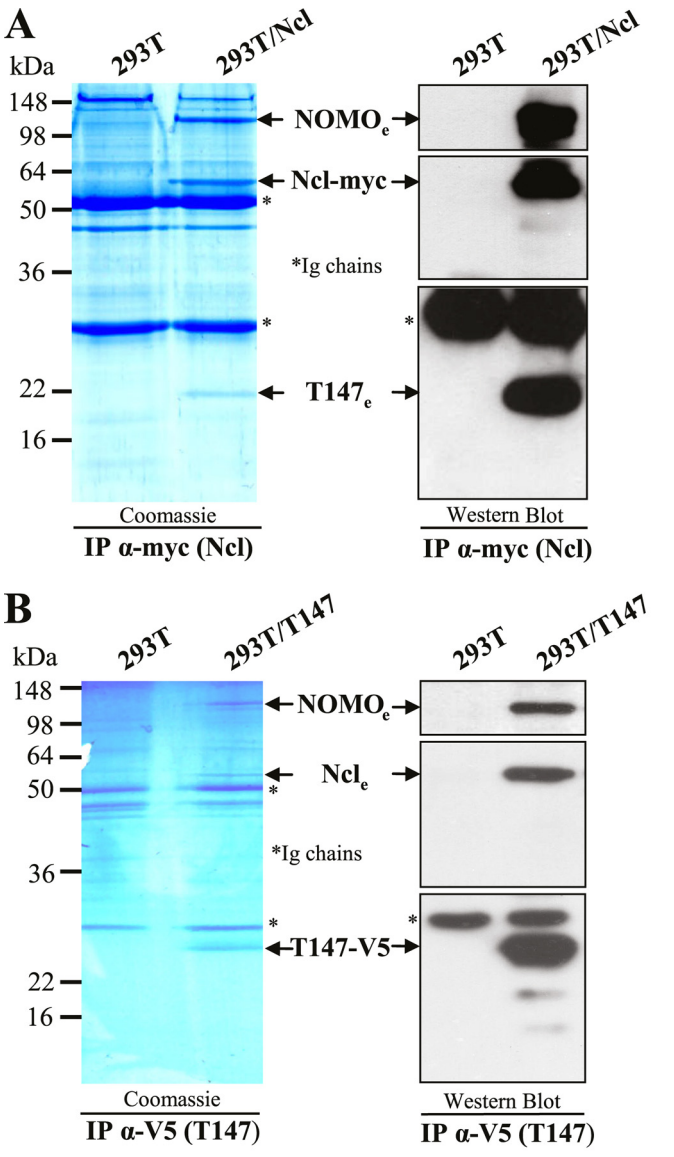

FIGURE 1. **TMEM147 is a major interactor of Nicalin and NOMO.** *A*, Nicalin-Myc (Ncl-Myc) was immunoprecipitated (*IP*) from large scale membrane preparations (detergent: 0.7% DDM), and the bound proteins were visualized by Coomassie Blue staining (*left panel*). In addition to NOMO (~130 kDa), an ~22-kDa band, identified as T147, was specifically enriched in precipitates from HEK293T/Ncl-Myc cells (bands denoted with * represent immunoglobulin heavy and light chains). Immunoblotting using a monoclonal anti-TMEM147 antibody confirmed its identity (*right panel*). *B*, immunoprecipitation of V5-tagged TMEM147 from overexpressing cells resulted in the specific enrichment of an ~60- and ~130-kDa band (*left panel*) identified as Nicalin and NOMO by immunoblotting (*right panel*). *C*, comparison of input, bound (*IP*), and unbound (*post IP*) material of Nicalin-Myc (*left panel*) and TMEM147-V5 (*right panel*) immunoprecipitations by immunoblotting. A strong enrichment of the respective binding partners (*middle lanes*) as well as their depletion in the post-immunoprecipitation supernatants (*right lanes*) is observed. No binding or depletion of the membrane protein calnexin is detectable. *e*, endogenous.

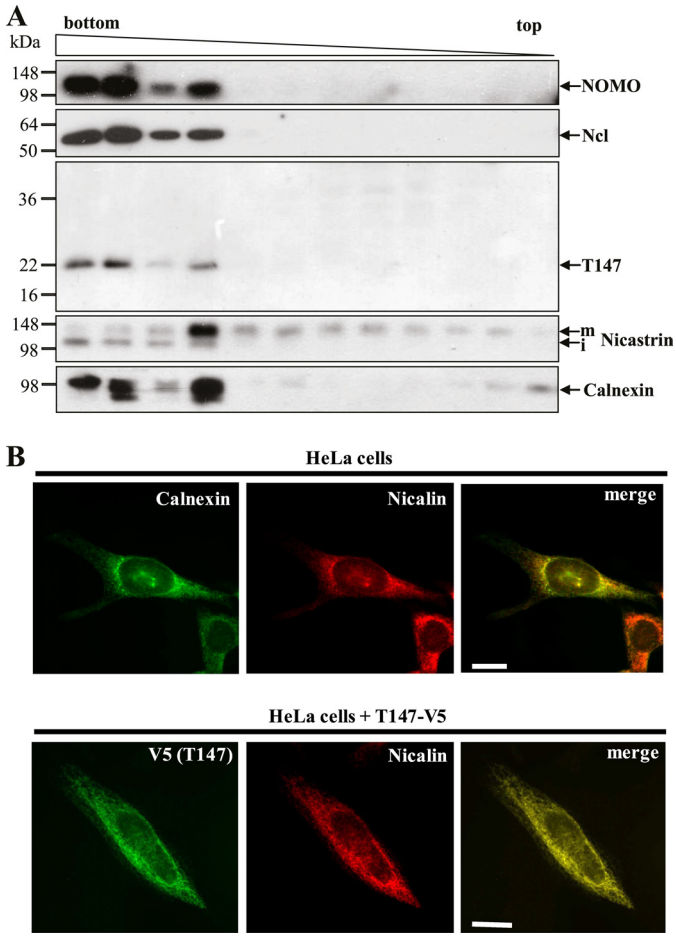

FIGURE 2. **TMEM147 colocalizes with Nicalin in the ER.** *A*, density gradient centrifugation using membrane protein lysates from HEK293T cells. Collected fractions were analyzed by immunoblotting. The distribution of TMEM147, Nicalin, and NOMO is highly similar with an exclusive presence in the four bottom fractions, which are enriched in ER membranes, as shown by the presence of the ER marker calnexin and of immature (*i*) Nicastrin. *m*, mature. *B*, immunofluorescence microscopy of wild-type HeLa cells and cells overexpressing V5-tagged TMEM147. Nicalin colocalizes with calnexin (*upper panel*) confirming the ER localization of endogenous Nicalin previously reported (11). Staining for TMEM147 in overexpressing cells resulted in a reticular pattern that largely overlapped with the Nicalin staining, demonstrating colocalization within the ER. (*Scale bars*, 10 μm.)

V5-tagged TMEM147 (endogenous TMEM147 levels in wild-type cells were below the detection limit). These results supported the fractionation data, and we concluded that TMEM147, like its binding partners Nicalin and NOMO, localizes to the ER membrane, supporting the idea that the three proteins are indeed components of the same complex.

TMEM147, Nicalin, and NOMO Stabilize Each Other—One prominent feature of Nicalin and NOMO is the tight control of their steady-state levels, which is a consequence of the stabilization of the protein monomers upon incorpora-

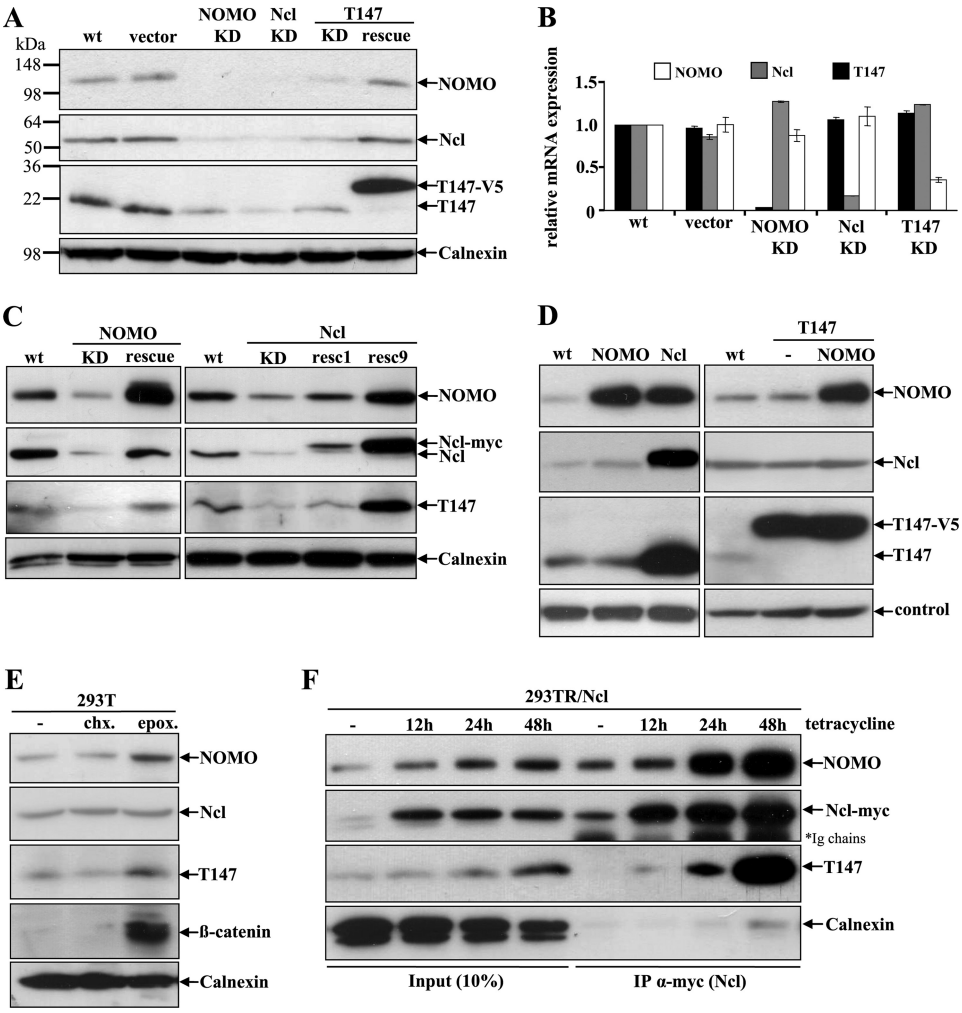

FIGURE 3. **TMEM147, Nicalin, and NOMO protein levels are mutually dependent.** *A*, HeLa cells were transduced with lentiviruses encoding the respective short hairpin RNAs to generate stable Nicalin, NOMO, and TMEM147 knockdown (*KD*) cell lines. Protein levels were analyzed by immunoblotting. The knockdown of Nicalin, NOMO, or TMEM147 resulted in a strong reduction of the respective binding partners. Stable reintroduction of an RNAi-resistant TMEM147 cDNA containing a V5 tag (T147 rescue) restored NOMO and Nicalin levels. *wt*, wild type. *B*, mRNA levels in HeLa knockdown cells were quantitated by real-time PCR showing a decrease in target gene expression by 75–90%. The mRNA levels of the interaction partners were only marginally changed. Shown are mean values from three experiments; *error bars* indicate standard deviations. *C*, knockdown (*KD*) and rescue of NOMO and Nicalin in HEK293T cells. TMEM147 expression is reduced in Nicalin and NOMO knockdown cell lines and restored in the rescue cell lines. In a high expression Nicalin rescue clone (*Ncl resc9*), NOMO and TMEM147 expression are dramatically increased. *D*, HEK293T cell lines stably overexpressing Nicalin, NOMO, and TMEM147. NOMO overexpression has no effect on Nicalin and TMEM147 levels, whereas Nicalin overexpression results in an increase in NOMO and TMEM147 levels. TMEM147 overexpression does not alter NOMO and Nicalin levels but results in the disappearance of endogenous TMEM147 (replacement). Even the simultaneous overexpression of TMEM147 and NOMO does not lead to an increase in Nicalin expression. Controls are calnexin (*left panel*) and β-actin (*right panel*). *E*, evidence for excess synthesis of TMEM147 and NOMO in HEK293T cells. Nicalin, NOMO, and TMEM147 immunoreactivities were not significantly changed upon ribosome inhibition (*chx.*, cycloheximide, 6 h), indicating a long half-life of the proteins under steady-state conditions. Proteasome inhibition (*epox.*, epoxomicin, 6 h) resulted in an increase in NOMO and TMEM147 levels, indicating the synthesis of excessive protein. *F*, kinetics of TMEM147 and NOMO stabilization and complex formation in cells with inducible Nicalin expression (293TR/Ncl). Induction of Nicalin expression by tetracycline for the indicated times led to a continuous increase in TMEM147 and NOMO levels over time in lysates (*four left lanes*) and Nicalin immunoprecipitates (*four right lanes*), demonstrating enhanced complex formation. The increase of NOMO appears to precede the elevation of TMEM147, an indication for a stepwise complex assembly.

tion into the complex (11). This becomes evident in RNAi studies in cultured cells where a knockdown of Nicalin results in a parallel reduction of NOMO and *vice versa*. To analyze whether TMEM147 is subject to the same stabilization mechanism, we used a lentivirus-based expression system in HeLa cells to generate cell lines stably expressing Nicalin-, NOMO-, or TMEM147-specific short hairpin RNAs. The mutual dependence of Nicalin and NOMO expression previously shown in HEK293T cells was confirmed, demonstrating that it is not cell type-specific (Fig. 3*A*). A similar dependence was observed for TMEM147; in Nicalin and NOMO knockdown cells, its expression was strongly reduced, and in TMEM147 knockdown cells, Nicalin and NOMO levels were decreased (Fig. 3*A*). These reductions in the protein expression levels were not accompanied by a decline in the corresponding mRNA expression levels as determined by quantitative real-time PCR (Fig. 3*B*). This not only confirmed previous data for Nicalin and NOMO (11) but also showed that the reduction in TMEM147 protein expression is caused by a posttranscriptional mechanism.

To demonstrate the reversibility of these effects, we used knockdown rescue cells generated by the introduction of the respective RNAi-resistant expression plasmids. The TMEM147 knockdown in HeLa cells was rescued by the expression of a V5-tagged version migrating at ~25 kDa and resulted in the restoration of Nicalin and NOMO levels (Fig. 3*A*). It also caused a further reduction of endogenous TMEM147, a phenomenon known as replacement (see below). For the Nicalin and NOMO rescue, we used the HEK293 cells described previously (11) and analyzed TMEM147 expression levels. They were found to be restored in both cell lines (Fig. 3*C*), further underlining the close association between the three proteins. In a high expressing Nicalin rescue clone (resc9), TMEM147 expression exceeded the wild-type levels severalfold, an observation we had already described for NOMO (11). Overexpression studies in wild-type HEK293T cells replicated this effect (Fig. 3*D*), and quantitative mRNA measurements demonstrated that the elevations in TMEM147 expression are not due to a rise in mRNA levels, again demonstrating a posttranscriptional cause (data not shown). TMEM147 as well as NOMO overexpression, either alone or in combination, did not result in elevated Nicalin levels (Fig. 3*D*). Thus, the regulation mechanism proposed recently (11) was confirmed and can now be extended to

TMEM147. TMEM147 and NOMO are synthesized in excess and rapidly degraded in wild-type cells. This is supported by the fact that proteasome inhibition by epoxomicin in wild-type cells resulted in increased TMEM147 and NOMO levels (Fig. 3*E*). Upon Nicalin overexpression, an increased number of TMEM147 molecules is stabilized by Nicalin binding, strongly corroborating the hypothesis that TMEM147 is a member of the Nicalin-NOMO complex.

Another consequence of the described stabilization mechanism is the so-called replacement, a phenomenon originally reported for Presenilin (12) and later also observed for Nicalin (11). In cells overexpressing Nicalin (or Presenilin), the levels of the endogenous protein are strongly reduced (Fig. 3*D*). This is thought to be a consequence of the incorporation of ectopic molecules into the complex at the expense of the endogenous counterparts, which are probably degraded (although this has never been demonstrated for Presenilin or Nicalin). We now observed replacement also for TMEM147 in knockdown rescue cells (Fig. 3*A*, *right lane*) as well as in overexpressing wild-type cells (Fig. 3*D*, *right panel*), underlining the similarity between the Nicalin-NOMO and the γ-secretase complex.

We have previously analyzed the kinetics of the NOMO stabilization through Nicalin by using a cell line in which Nicalin expression can be induced by tetracycline (11). In these cells, a continuous increase in NOMO protein levels occurs over time upon tetracycline treatment until NOMO has finally adapted to Nicalin levels more than 24 h after Nicalin induction. We have now analyzed endogenous TMEM147 levels in these cells and observed an elevation with similar kinetics (Fig. 3*F*). This was accompanied by an enhanced interaction with Nicalin as shown by co-immunoprecipitation, confirming that Nicalin represents the key regulator of the complex. However, the increase in TMEM147 expression appeared to lag behind that of NOMO, which might indicate that the complex assembly occurs in a stepwise manner (see below).

TMEM147 and NOMO Bind to Different Nicalin Domains—In addition to the altered kinetics of TMEM147 and NOMO in the time course experiment, we noticed differences in their binding behavior. In Nicalin immunoprecipitates from Nonidet P-40-containing protein lysates, NOMO but not TMEM147 was detected (Fig. 4*A*), indicating different binding characteristics. Of note, Nonidet P-40 (*NP-40*) is known to completely disrupt γ-secretase, a membrane protein complex where the complex components are believed to interact mainly by transmembrane domains (16). This prompted us to analyze the Nicalin domains, which might mediate the interaction with NOMO and TMEM147 by expressing Nicalin deletion constructs (Fig. 4*B*) in HEK293T cells and analyzing their ability to increase NOMO and TMEM147 levels as indication of their binding competence. Expression of Nicalin lacking its cytosolic C terminus (NclΔC) resulted in an increase of both NOMO and TMEM147 levels to a similar extent, although less efficiently than the full-length protein (Fig. 4*C*). Nicalin lacking both cytosolic C terminus and transmembrane domain (NclΔTMC) only stabilized NOMO, leaving TMEM147 expression levels unchanged. Similar results were obtained from a Nicalin knockdown rescue study, where the stable introduction of RNAi-insensitive NclΔTMC restored NOMO but not TMEM147 expression (Fig. 4*D*). These findings indicated that the Nicalin transmembrane domain is essential for TMEM147 but dispensable for NOMO interaction.

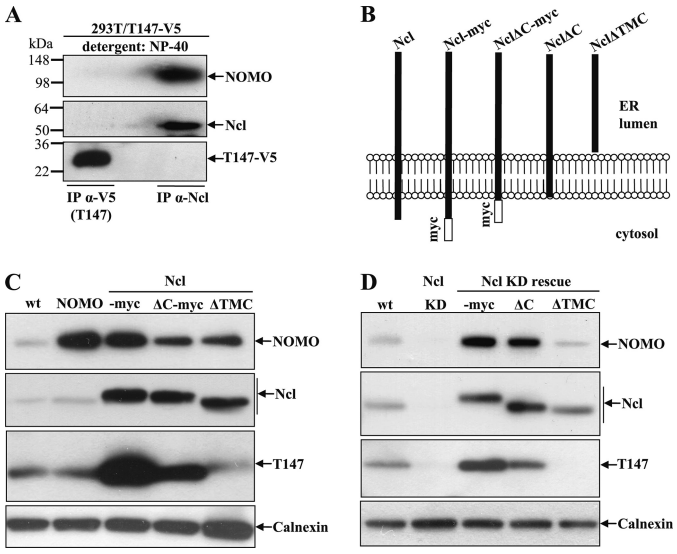

FIGURE 4. **TMEM147 and NOMO bind to different Nicalin domains.** *A*, Nonidet P-40 (*NP-40*) partially disrupts the complex. Membrane protein lysates containing 1% Nonidet P-40 as detergent were generated from 293T/TMEM147-V5 cells. In TMEM147 immunoprecipitates (*IP*) NOMO and Nicalin could not be detected (*left lane*), whereas in Nicalin immunoprecipitates TMEM147 was not found (*right lane*). *B*, a schematic illustration of the Nicalin deletion mutants analyzed. *C*, the Nicalin transmembrane domain is essential for TMEM147 but dispensable for NOMO binding. Nicalin-Myc and the deletion mutants NicalinΔC-Myc and NicalinΔTMC were stably expressed in HEK293T cells, and their effects on NOMO and TMEM147 levels were analyzed (in comparison with wild-type (*wt*) and NOMO-expressing cells). Whereas NicalinΔC was able to elevate both NOMO and TMEM147, although with a lower efficiency than Nicalin-Myc, in NicalinΔTMC-expressing cells, only NOMO was increased. *D*, RNAi-insensitive Nicalin-Myc, NicalinΔC, and NicalinΔTMC constructs were stably expressed in HEK293T/Nicalin knockdown (*KD*) cells. The ability of the Nicalin variants to restore NOMO and TMEM147 expression was analyzed by immunoblotting (when compared with wild-type and Nicalin knockdown cells). NicalinΔC was able to rescue NOMO and TMEM147 expression but was less efficient in elevating it beyond wild-type levels than Nicalin-Myc. In contrast, NicalinΔTMC restored NOMO to wild-type levels but was unable to restore TMEM147 expression.

The Developmental Expression of TMEM147 Is Similar to Nicalin and NOMO—Nicalin, NOMO, and TMEM147 orthologs are present in all multicellular organisms with a high degree of sequence conservation and almost identical lengths (Fig. 5*A*), suggesting that the interaction between these proteins might be conserved. We tested this by stably expressing zebrafish Nicalin (zfNicalin) in HEK293T cells and analyzing protein levels by immunoblotting. Endogenous TMEM147 and NOMO levels were increased and endogenous human Nicalin expression was reduced, demonstrating replacement (Fig. 5*B*) and indicating that the zfNicalin is functional in human cells. To show this more directly, we overexpressed Myc-tagged zebrafish TMEM147 and performed anti-Myc immunoprecipitation from membrane protein lysates. We detected co-precipitation of endogenous Nicalin and NOMO, demonstrating that the interaction is conserved. zfTMEM147 expression also led to replacement of endogenous TMEM147, further showing its functionality (data not shown). These results strongly suggested that the interaction of TMEM147 with the Nicalin-NOMO complex is evolutionary conserved.

A

	% Identity to human			length (aa)		
	Ncl	NOMO	T147	Ncl	NOMO	T147
H.sapiens	100	100	100	563	1222	224
M.musculus	93	93	99	563	1214	224
X.laevis	81	79	78	560	1206	225
D.rerio	74	71	78	572	1208	225
D.melanogaster	35	32	49	561	1199	227
C.elegans	31	26	42	563	1121	225
A.thaliana	33	30	38	565	1227	228

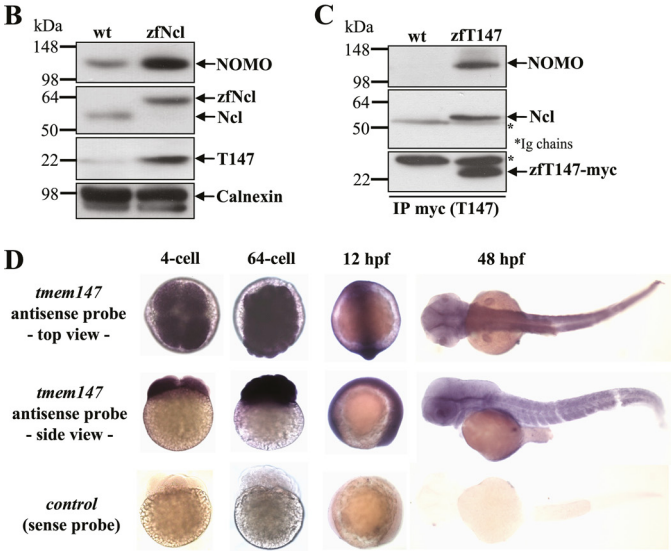

FIGURE 5. **The interaction between Nicalin, NOMO, and TMEM147 is evolutionary conserved.** *A*, the percentage of amino acid (*aa*) identity (based on FASTA alignment) and lengths (in amino acids) of Nicalin, NOMO, and TMEM147 orthologs in selected multicellular organisms are shown. *H.sapiens*, *Homo sapiens*; *M.musculus*, *Mus musculus*; *X. laevis*, *Xenopus laevis*; *D. rerio*, *Danio rerio*; *D.melanogaster*, *Drosophila melanogaster*; *A.thaliana*, *Arabidopsis thaliana*. *B*, effect of zebrafish Nicalin (*zfNcl*) on the expression of the human orthologs. zfNicalin was stably expressed in HEK293T cells and resulted in the disappearance of endogenous Ncl and in the elevation of endogenous NOMO and TMEM147 levels. Note that zfNicalin migrates slightly higher than human Nicalin and that the amount of overexpressed zfNicalin is underestimated due to a lower affinity of the antibody. *wt*, wild type. *C*, zebrafish TMEM147 (*zfT147*) interacts with human complex partners. Immunoprecipitation of Myc-tagged zfTMEM147 from overexpressing cells resulted in the specific enrichment of endogenous human Nicalin and NOMO. *D*, zebrafish TMEM147 is expressed during embryonic development. *In situ* hybridization revealed maternal expression (four-cell stage) and ubiquitous zygotic expression of *tmem147* mRNA in fixed zebrafish embryos. The lack of a labeling with the sense probe demonstrated the specificity of the antisense probe. *hpf*, hours post fertilization.

During zebrafish development, Nicalin and NOMO are expressed maternally and throughout early embryonic stages, in agreement with their proposed role in Nodal signaling (10). To analyze the expression pattern of *tmem147* mRNA, we performed *in situ* hybridization in fixed embryos at different stages. We found maternal and zygotic expression of *tmem147* mRNA throughout the first 48 h of development (Fig. 5*D*). At 12 and 48 h after fertilization, no tissue- or organ-specific expression but rather ubiquitous expression was detected. Similar spatiotemporal expression patterns were shown for zfNicalin and zfNOMO (10), further suggesting that the interaction between TMEM147 and the Nicalin-NOMO complex is functionally relevant.

DISCUSSION

In the present study, we explored the possibility that the Nicalin-NOMO membrane protein complex contains additional protein components. The use of a modified Nicalin affinity purification procedure allowed the co-isolation of an ~22-kDa protein from human HEK293T cells that was identified as TMEM147 by mass spectrometry analysis. Like Nicalin and NOMO, it is highly conserved in metazoans, expressed ubiquitously, and localizes to the endoplasmic reticulum. Co-precipitation/immunoblotting experiments confirmed the interaction and demonstrated that all three proteins are major binding partners. We subsequently collected a variety of data suggesting that TMEM147 is a genuine component of the Nicalin-NOMO complex. First, the combined molecular sizes of Nicalin (60 kDa), NOMO (130 kDa), and TMEM147 (22 kDa) are in good agreement with the native size of the complex (200–220 kDa) as determined by Blue-Native-PAGE (11). Second, all three proteins colocalize in the endoplasmic reticulum. Third, the reduction of one of the proteins results in the destabilization of the other two. Fourth, Nicalin controls the expression levels of both TMEM147 and NOMO. Fifth, the interaction between Nicalin and TMEM147 is evolutionary conserved, and the expression patterns of all three proteins during zebrafish development are highly similar.

The regulatory role of Nicalin in the assembly of the complex proposed previously (11) could be confirmed and extended. We show that Nicalin not only controls NOMO, but also TMEM147 expression levels, corroborating the idea that it represents the rate-limiting factor. It most likely acts by binding and stabilizing TMEM147 and NOMO molecules, which are synthesized in excess and subject to a rapid turnover through proteolytic degradation in their monomeric form.

We further find indications for a sequential assembly of the Nicalin-NOMO complex; a subcomplex consisting only of Nicalin and NOMO can be immunoisolated under certain detergent conditions, and upon induced expression of Nicalin, the stabilization of NOMO appears to precede that of TMEM147. In addition, we show that different Nicalin domains mediate the interactions with the two binding partners; although the luminal domain is sufficient for the interaction with NOMO, the transmembrane domain is required for the interaction with TMEM147. These findings fit into a model in which the formation of a Nicalin-NOMO subcomplex, mediated by their luminal domains, initiates complex assembly followed by the binding of TMEM147 to the Nicalin transmembrane region. TMEM147 is predicted to represent a polytopic protein containing seven transmembrane domains, with its N terminus residing in the ER lumen and its C terminus facing the cytosolic side of the membrane, a topology highly reminiscent of the γ-secretase component APH-1 (35) (supplemental Fig. S1). It is tempting to speculate that TMEM147 and APH-1 might play similar roles in the assembly of their respective complexes. However, although the assembly of γ-secretase is initiated by an APH-1-Nicastrin subcomplex (18), TMEM147 does not appear to be involved in the initial step of the formation of the Nicalin-NOMO complex, indicating different assembly modes. Nevertheless, both complexes are likely generated in a stepwise manner, and TMEM147 and APH-1 are essential factors in this process.

We have previously reported the antagonistic effect of the Nicalin-NOMO complex on the Nodal signaling pathway

(10). *In situ* hybridization experiments revealed that TMEM147 is expressed in a similar spatiotemporal pattern during zebrafish development, underlining the functional relevance of the identified interaction with the Nicalin-NOMO complex. However, Nodal signaling is believed to be restricted to processes during pregastrulation and gastrulation stages of chordate development (31), and we detected expression of all complex components also at later stages. Moreover, they are widely expressed in various human and mouse cell lines (Ref. 11 and data not shown). Finally, the Nodal signaling pathway exists only in vertebrates, but orthologs of Nicalin, NOMO, and TMEM147 are also present in invertebrates, indicating that the complex might fulfill additional functions. Interestingly, recent data suggest an involvement of the complex in invertebrate nicotinic acetylcholine receptor (nAChR) assembly (32, 33). nAChRs are homo- or heteropentameric ligand-gated ion channels involved in excitatory neurotransmission and muscle activation. By tandem affinity purification of *Caenorhabditis elegans* nAChRs, ceNicalin (nra-2) and ceNOMO (nra-4) were co-isolated (32). In ceNicalin and ceNOMO loss-of-function mutant animals, synaptic nAChR subunit composition and function were affected, and ceNicalin mutant phenotypes could be partially rescued by expression of the human ortholog (33). Based on these data and the localization of ceNicalin and ceNOMO to the endoplasmic reticulum, it was proposed that the complex is involved in the assembly and the subunit selection of nAChRs. However, due to differences in vertebrate and invertebrate nAChR systems (34), the relevance of these findings for vertebrates requires further investigation. ceTMEM147 was not identified by this approach, which can be interpreted in two ways. Either it is not required for the function of the Nicalin-NOMO complex in *C. elegans*, or it was missed in the purification procedure. Based on our own difficulties to identify TMEM147 in a less complex purification approach, we favor the latter possibility and believe that TMEM147 is a genuine component of the Nicalin-NOMO complex in all species. However, the generation of further tools is required to elucidate the details of its function, most importantly loss-of-function animal models, especially in vertebrates. Our studies suggest that it is sufficient to target only one of the three genes to eliminate the complex. Likewise, a gain-of-function should be achieved solely by increasing the expression of Nicalin. These studies will not only contribute to the understanding of the function of the Nicalin-NOMO complex but might also help to elucidate general mechanisms involved in the assembly of membrane protein complexes.

Acknowledgments—We thank Dr. Ignasi Forné from the Zentrallabor für Proteinanalytik (ZfP) for support with the mass spectrometry analysis.

REFERENCES

1. Selkoe, D., and Kopan, R. (2003) *Annu. Rev. Neurosci.* **26,** 565–597
2. Haass, C., and Selkoe, D. J. (2007) *Nat. Rev. Mol. Cell Biol.* **8,** 101–112
3. Wolfe, M. S., Xia, W., Ostaszewski, B. L., Diehl, T. S., Kimberly, W. T., and Selkoe, D. J. (1999) *Nature* **398,** 513–517
4. Yu, G., Nishimura, M., Arawaka, S., Levitan, D., Zhang, L., Tandon, A., Song, Y. Q., Rogaeva, E., Chen, F., Kawarai, T., Supala, A., Levesque, L., Yu, H., Yang, D. S., Holmes, E., Milman, P., Liang, Y., Zhang, D. M., Xu, D. H., Sato, C., Rogaev, E., Smith, M., Janus, C., Zhang, Y., Aebersold, R., Farrer, L. S., Sorbi, S., Bruni, A., Fraser, P., and St George-Hyslop, P. (2000) *Nature* **407,** 48–54
5. Francis, R., McGrath, G., Zhang, J., Ruddy, D. A., Sym, M., Apfeld, J., Nicoll, M., Maxwell, M., Hai, B., Ellis, M. C., Parks, A. L., Xu, W., Li, J., Gurney, M., Myers, R. L., Himes, C. S., Hiebsch, R., Ruble, C., Nye, J. S., and Curtis, D. (2002) *Dev. Cell.* **3,** 85–97
6. Goutte, C., Tsunozaki, M., Hale, V. A., and Priess, J. R. (2002) *Proc. Natl. Acad. Sci. U.S.A.* **99,** 775–779
7. Shah, S., Lee, S. F., Tabuchi, K., Hao, Y. H., Yu, C., LaPlant, Q., Ball, H., Dann, C. E., 3rd, Südhof, T., and Yu, G. (2005) *Cell* **122,** 435–447
8. Chávez-Gutiérrez, L., Tolia, A., Maes, E., Li, T., Wong, P. C., and de Strooper, B. (2008) *J. Biol. Chem.* **283,** 20096–20105
9. Dries, D. R., Shah, S., Han, Y. H., Yu, C., Yu, S., Shearman, M. S., and Yu, G. (2009) *J. Biol. Chem.* **284,** 29714–29724
10. Haffner, C., Frauli, M., Topp, S., Irmler, M., Hofmann, K., Regula, J. T., Bally-Cuif, L., and Haass, C. (2004) *EMBO J.* **23,** 3041–3050
11. Haffner, C., Dettmer, U., Weiler, T., and Haass, C. (2007) *J. Biol. Chem.* **282,** 10632–10638
12. Thinakaran, G., Harris, C. L., Ratovitski, T., Davenport, F., Slunt, H. H., Price, D. L., Borchelt, D. R., and Sisodia, S. S. (1997) *J. Biol. Chem.* **272,** 28415–28422
13. Zhang, Y. W., Luo, W. J., Wang, H., Lin, P., Vetrivel, K. S., Liao, F., Li, F., Wong, P. C., Farquhar, M. G., Thinakaran, G., and Xu, H. (2005) *J. Biol. Chem.* **280,** 17020–17026
14. Edbauer, D., Winkler, E., Haass, C., and Steiner, H. (2002) *Proc. Natl. Acad. Sci. U.S.A.* **99,** 8666–8671
15. Lee, S. F., Shah, S., Li, H., Yu, C., Han, W., and Yu, G. (2002) *J. Biol. Chem.* **277,** 45013–45019
16. LaVoie, M. J., Fraering, P. C., Ostaszewski, B. L., Ye, W., Kimberly, W. T., Wolfe, M. S., and Selkoe, D. J. (2003) *J. Biol. Chem.* **278,** 37213–37222
17. Hu, Y., and Fortini, M. E. (2003) *J. Cell Biol.* **161,** 685–690
18. Takasugi, N., Tomita, T., Hayashi, I., Tsuruoka, M., Niimura, M., Takahashi, Y., Thinakaran, G., and Iwatsubo, T. (2003) *Nature* **422,** 438–441
19. Kim, S. H., Yin, Y. I., Li, Y. M., and Sisodia, S. S. (2004) *J. Biol. Chem.* **279,** 48615–48619
20. Capell, A., Beher, D., Prokop, S., Steiner, H., Kaether, C., Shearman, M. S., and Haass, C. (2005) *J. Biol. Chem.* **280,** 6471–6478
21. Rupp, R. A., Snider, L., and Weintraub, H. (1994) *Genes Dev.* **8,** 1311–1323
22. Krüger, M., Kratchmarova, I., Blagoev, B., Tseng, Y. H., Kahn, C. R., and Mann, M. (2008) *Proc. Natl. Acad. Sci. U.S.A.* **105,** 2451–2456
23. Shevchenko, A., Tomas, H., Havlis, J., Olsen, J. V., and Mann, M. (2006) *Nat. Protoc.* **1,** 2856–2860
24. Mullins, M. C., Hammerschmidt, M., Haffter, P., and Nüsslein-Volhard, C. (1994) *Curr. Biol.* **4,** 189–202
25. Kimmel, C. B., Ballard, W. W., Kimmel, S. R., Ullmann, B., and Schilling, T. F. (1995) *Dev. Dyn.* **203,** 253–310
26. Thisse, C., Thisse, B., Schilling, T. F., and Postlethwait, J. H. (1993) *Development* **119,** 1203–1215
27. Wiznerowicz, M., and Trono, D. (2003) *J. Virol.* **77,** 8957–8961
28. Lois, C., Hong, E. J., Pease, S., Brown, E. J., and Baltimore, D. (2002) *Science.* **295,** 868–872
29. Winkler, E., Hobson, S., Fukumori, A., Dümpelfeld, B., Luebbers, T., Baumann, K., Haass, C., Hopf, C., and Steiner, H. (2009) *Biochemistry* **48,** 1183–1197
30. Viklund, H., and Elofsson, A. (2004) *Protein Sci.* **13,** 1908–1917
31. Shen, M. M. (2007) *Development* **134,** 1023–1034
32. Gottschalk, A., Almedom, R. B., Schedletzky, T., Anderson, S. D., Yates, J. R., 3rd, and Schafer, W. R. (2005) *EMBO J.* **24,** 2566–2578
33. Almedom, R. B., Liewald, J. F., Hernando, G., Schultheis, C., Rayes, D., Pan, J., Schedletzky, T., Hutter, H., Bouzat, C., and Gottschalk, A. (2009) *EMBO J.* **28,** 2636–2649
34. Jones, A. K., Davis, P., Hodgkin, J., and Sattelle, D. B. (2007) *Invert. Neurosci.* **7,** 129–131
35. Fortna, R. R., Crystal, A. S., Morais, V. A., Pijak, D. S., Lee, V. M., and Doms, R. W. (2004) *J. Biol. Chem.* **279,** 3685–3693